



# Sour cherry seed proteins devoted to covalently bonded carbohydrate moieties: efficacy of transaction and carbohydrate type on amino acid distribution and emulsifier behavior

Merve Akalan<sup>1</sup> · Bülent Başyigit<sup>1</sup> · Melike Yücepete<sup>1</sup> · Mehmet Şükrü Karakuş<sup>1</sup> · Kamile Bayrak Akay<sup>1</sup> · Asliye Karaaslan<sup>2</sup> · Mehmet Karaaslan<sup>1</sup>

Received: 5 March 2023 / Accepted: 21 December 2023 / Published online: 3 February 2024

© The Author(s) 2024

## Abstract

This paper handled the Maillard reaction under controlled conditions to conjugate sour cherry seed protein isolate (SCPI) with gum Arabic (GA), carboxymethyl cellulose (CMC), and pectin (P) polysaccharides. Characteristic investigations for conjugates were conducted by browning intensity, glycation degree, amino acid, FTIR, SEM, and TGA analyses. After glycation, the level of lysine and arginine declined. Conjugation process displayed beneficial efficacy on techno-functional attributes, namely solubility, water holding capacity, oil holding capacity, foaming capacity/stability and emulsion activity/stability of SCPI but maximum values in terms of these attributes were variable according to conjugate type. Stability index of emulsions stabilized by using conjugates including SCPI-GA (0.87 R), SCPI-CMC (0.94 R), and SCPI-P (0.95 R) was superior than that of SCPI alone (0.60 R). Centrifugal precipitation rate was 59.17, 36.04, 32.61, and 30.92% for emulsions prepared in the presence of SCPI, SCPI-GA, SCPI-CMC, and SCPI-P, respectively. Resilience to freeze-thawed, pH-shifting, various salt concentrations, and different temperature applications of emulsions were investigated to evaluate emulsifier behavior of protein and conjugates in food systems. Findings showed that emulsifying properties of the conjugates prepared using P and CMC came to the fore compared to SCPI alone and SCPI-GA.

**Keywords** Sour cherry seed protein · Maillard reaction · Protein-polysaccharide conjugates · Amino acid · Techno-functional properties · Resilience to environmental stress

## Introduction

Protein synthesis involves the conversion of hereditary genetic information into the precisely sequenced amino acid chains. Proteins are the fundamental structural and functional biomaterials of cells and each protein is made of by certain number of amino acid residues arranged in an ordered fashion. Living organisms synthesize their intrinsic proteins by combining a variety of amino acids. A balanced and healthy diet should contain complete proteins rather than excessive processed carbohydrates. It is estimated that global

protein requirement will be increased two times by 2050. Other than structural and regulatory missions, proteins are used to fulfill specific foaming, water/oil holding, emulsifying, gelling and filming assignments in food/biomaterial production.

Adequate protein intake to body is a requirement for the continuation of life activities. Human beings mostly meet their protein needs by consuming animal-based foods, *e.g.* fish, milk, meat, and eggs [1]. However, these sources are not suitable for private consumers including people with a vegan/vegetative diet and celiac disease. Over and above, carbon footprint, environmental uncleanliness, and animal welfare are other problems. Another point that should not be overlooked in this respect is the prejudice against animal sources, especially because of their negative effects on health [2]. Nevertheless, protein market has been expanding rapidly, recently. Therefore, it is essential to find alternative sources to respond to this market. Scientific literature and industry are focused

✉ Mehmet Karaaslan  
mk385@cornell.edu

<sup>1</sup> Food Engineering Department, Engineering Faculty, Harran University, Şanlıurfa, Turkey

<sup>2</sup> Vocational School, Food Processing Programme, Harran University, Şanlıurfa, Turkey

on the plant-based proteins for limiting the consumption of animal-based ones and overcoming the stated problems. For this reason, global prevalence of plant-based proteins has increased at last decade. Grains (millet, wheat, sorghum, rice, and barley), legumes (soybean, red mullet, lupin, pea, faba beans, pigeon pea, chickpea, and cowpea), and oilseeds (sesame, flaxseed, rapeseed, chia, pumpkin, and cottonseed) are the leading sources of plant-based proteins [2, 3]. However, some drawbacks arise when proteins obtained by using these raw materials are intaken to the body. A simple example of this is allergenicity, which is an earnest health problem. Previous studies outlined the allergenic attribute of soy and pea proteins [4, 5]. Thus, efforts to identify novel and innovative plant-based protein sources are being conducted. In this context, in parallel with waste management, studies have been engaged to obtain plant-based proteins from food processing by-products and use them for different aims [6]. On the other hand, it was stated in previous studies that plant-based proteins are not at the level of animal-based counterparts in terms of techno-functional behaviors [7]. Current knowledge shows that the lack of these abilities is considerable obstacle to the evaluation of plant-derived proteins in the industry. This deficiency could be eliminated by being modified the natural structure of proteins with various approaches. Core of improving protein functional attributes is physical, chemical, and enzymatic implementations [8]. The Maillard reaction is one of the most common techniques utilized in protein modification. This chemical process enables the amino groups (proteins, peptides, or amino acids) for binding to reducing carbonyl groups of sugars in the presence of temperature application [9]. The Maillard reaction was found to be promising way for developing the functional properties (from emulsification behaviors to thermal behaviors) of proteins [10, 11]. Gum Arabic, pectin and carboxymethyl cellulose can be given as examples for the polysaccharide side of reaction [12]. These carbohydrates are easy to access as well as non-toxic, modifiable, and biocompatible. However, gum Arabic, pectin and carboxymethyl cellulose likely behave differently in the reaction because of their distinctive nature. For this, specific focuses of this study were to conjugate sour cherry seed-based proteins (SCPI) with gum Arabic (GA), pectin (P) and carboxymethyl cellulose (CMC) via the Maillard reaction for improving the techno-functional properties of SCPI, investigate the suitable carbohydrate type for conjugation process, and evaluate emulsifier behaviors of synthesized conjugates under stress conditions (centrifugal forces, freeze–thaw, different pH, different salt concentrations, and different temperature).

## Materials and methods

### Materials

Sour cherry seeds were obtained from Mavi Deniz Food Inc. company in Isparta, Turkey. All chemicals including GA, CMC, and P were purchased from Sigma or Merck.

### Protein extraction process

SCPI extraction was performed as in our previous study [6] and the visual images related to the process steps are given in Fig. 1A. Firstly, the oil of the sour cherry seeds was separated by a laboratory-scale cold press machine (750 W power, 12 kg sample/h capacity and single head). Then, 10 g the defatted sour cherry seeds were mixed with 290 mL of distilled water. The pH of the solution was adjusted to 7.73 with 1 mol/L HCl or 1 mol/L NaOH and the solution volume was completed to 300 mL. The solutions were thoroughly mixed in a shaker for 63 min. At the end of the period, the samples were centrifuged at 4000 rpm for 10 min at +4 °C. After centrifugation, the pH of the supernatant was adjusted to 4.50 using 1 mol/L HCl or 1 mol/L NaOH for isoelectric precipitation. The precipitated proteins were dried using the freeze-drying (Coolermed, Türkiye) method. Proteins were stored in the refrigerator.

### Maillard conjugates preparation

One g polysaccharide (GA, CMC, and P) and 2 g SCPI were mixed homogeneously in 0.2 M sodium phosphate buffer solution (pH 7.0) in a glass 100 mL bottle for 2 h at room temperature. pH of solutions was adjusted to 7.0 using 0.1 M NaOH or 0.1 M HCl. After solutions were kept in the refrigerator overnight, they were held at 90 °C for 15 min for the Maillard reaction process [13]. At the end of the period, the cooled solutions were centrifuged at 4000 rpm at 4 °C for 10 min and dried by using freeze dryer (Coolermed, Türkiye).

### Browning intensity

Browning intensity of the Maillard conjugates was measured according to the method of Zhang et al. [14] with minor modification. Samples were diluted 50-fold using distilled water and their absorbance was measured using a UV–Vis spectrophotometer (Shimadzu, Kyoto, Japan) at 420 nm for browning intensity.

### Glycation degree

Glycation degree of samples was determined by quantifying the percentage of free amino groups. Free amino groups were quantified by OPA method with minor modifications

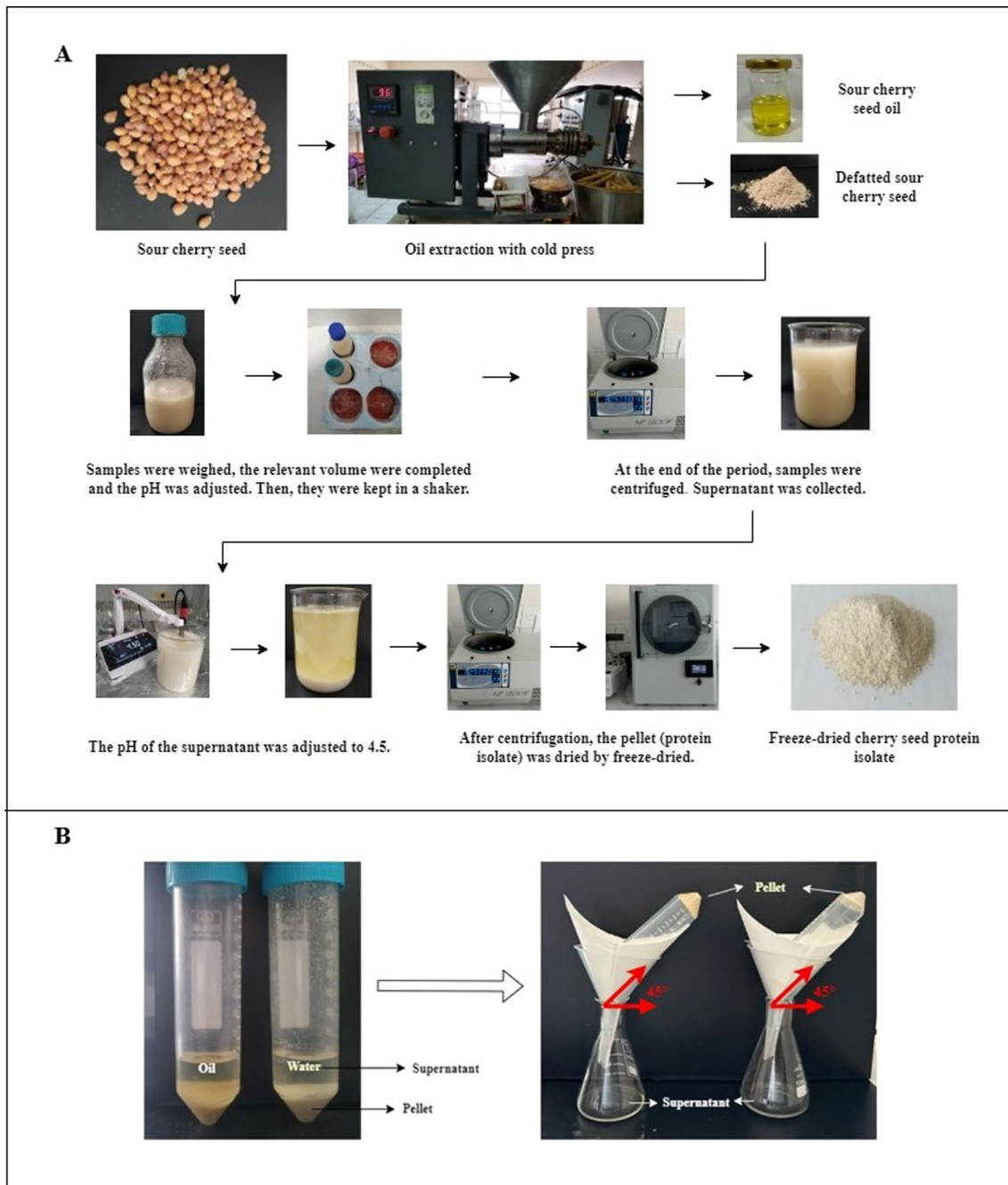


**Fig. 1** Flow chart of sour cherry seed protein extraction process (**A**) and supernatant separation for measurement of water and oil holding capacity (**B**)

[14]. OPA reagent was prepared by mixing 40 mg OPA (dissolved in 1 mL methanol), 25 mL borax solution (0.1 mol/L), 2.5 mL SDS solution (20%, w/v) and 100  $\mu$ L  $\beta$ -mercaptoethanol, and then added distilled water to 50 mL. A 0.2 mL distilled water containing 0.4 mg conjugate was reacted with 4 mL OPA reagent for 2 min at 35  $^{\circ}$ C. Absorbance was read at the wavelength of 340 nm with a UV-Vis spectrophotometer (Shimadzu, Kyoto, Japan).

Glycation degree was calculated using the equation as follows (Eq. (1)).

$$\text{Glycation degree (\%)} = \frac{A_0 - A_t}{A_0} * 100 \quad (1)$$

where,  $A_0$  represents absorbance of protein alone;  $A_t$  represents absorbance of conjugates.

## FTIR spectroscopy

Fourier transform infrared spectroscopy (FTIR) analysis was performed by an IRTracer100 (EN230V) spectrometer (Shimadzu Corporation., Kyoto, Japan) to determine protein-polysaccharide interaction. Scans were performed between 500 and 4000 wavelengths and resolution of 1/cm [6].

## Amino acid content

Sample hydrolyzation process was conducted according to a previous study with slight modifications [15]. Glass tubes containing the mixture of 0.5 g sample and 5 mL HCl (6 M) were kept at 110 °C for 24 h. After centrifugation at 5000 rpm for 30 min at 4 °C, dilutions (1:100, v/v) of these mixtures were prepared. Diluted samples were filtered using a 0.22 µm PTFE filter. Commercial kit protocol (Trimaris) was applied for the filtrates followed injected into LCMS-8045 (Shimadzu Corporation., Kyoto, Japan). A binary gradient pump, an autosampler (SIL-20AC), a degasser (DGU-20A3R), and a column thermostat (CTO-10ASVP) were parts of the related device. A Trimaris Amino Acid LC-MS/MS column (250 mm × 2 mm, 3 µm) was used for separation process. Mobile phase was 0.05% formic acid in water and its ratio was 30% in isocratic system. Acetonitrile constituted the remainder of mobile phase. Flow rate was adjusted as 0.07 µL/min. Other parameters namely column temperature (30 °C), injection volume (40 µL), desolvation line (300 °C), heat (500 °C), nebulizing gas (3 L/min), and drying gas (20 L/min) were fixed during analysis period [16].

## SEM images

Scanning electron microscopy (SEM) (Zeiss Sigma 300, Zeiss Co., Oberkochen, Germany) was used to examine the microstructure and surface morphology of protein and conjugates. Samples were first frozen in liquid nitrogen. Then, the coating process was carried out with the plasma formed on the pure gold target in an EMS coating device (15 kV, 2.5 min) at a thickness of 5 nm [17].

## Thermal analysis (TGA)

Thermal behavior of protein and conjugates was measured by Thermogravimetric Analyzer DTG-60 H (Shimadzu Corporation, Kyoto, Japan) operating at a heating rate of 10 °C/min from 30 °C to 1000 °C in an inert atmosphere (N<sub>2</sub>) [18].

## Solubility

Solubility of protein and conjugates was determined according to the method of Bradford [19]. Protein and conjugates

were dispersed in 10 mM phosphate buffer pH 7.0 (1 mg/mL), and stirred for 30 min at room temperature. Next, samples were filtered through Whatman Filter Paper (Cat #1003-090). Absorbance of solutions was recorded at 595 nm and protein concentration was calculated using a standard curve.

## Oil/water holding capacity

Ten mL corn oil for oil holding capacity and 10 mL distilled water for water holding capacity were added into containers weighing one gram sample. Samples were mixed for 1 h by vortexing for 10 s every 15 min at room temperature. At the end of the period, it was centrifuged at 4000 rpm for 15 min. Centrifuge tube was filtered at a 45° angle onto filter paper for 30 min to separate the supernatant and the actual images concerned to the separation steps are presented in Fig. 1B. Samples were weighed and their weights recorded. OHC and WHC were calculated as ratio of final weight of samples to initial weight [20].

## Foaming capacity and foaming stability

Fifty mL protein or conjugate solutions (1%, w/v) were homogenized in a 100 mL measuring cylinder for 1 min at 12,000 rpm. Volume values read before and after homogenization were noted. Foam capacity and foaming stability were determined according to the following equations (Eq. (2, 3)).

$$\text{Foaming capacity}(\%) = \frac{(V_2 - V_1)}{V_1} * 100 \quad (2)$$

$$\text{Foaming stability}(\%) = \frac{V_r}{V_2} * 100 \quad (3)$$

where  $V_1$  is the solution volume before homogenization,  $V_2$  is the solution volume after homogenization, and  $V_r$  is the solution volume after homogenization after 10 min [20].

## Emulsion activity and emulsion stability

Protein or conjugate samples were dissolved at 0.5% (w/v) in potassium phosphate buffer (pH 7.0, 10 mM). Oil-in-water emulsions were acquired by mixing corn oil (25%, v/v) into the solution and homogenized for 1 min at 12,000 rpm using Ultra-Turrax homogenizer [21].

For emulsion activity index (EAI), 50 µL emulsion was mixed with 5 mL of SDS solution (0.1%, v/v). Absorbance of this mixture was read at 500 nm. The following equation (Eq. (4)) was used to determine EAI.

$$\text{EAI} \left( \frac{m^2}{g} \right) = \frac{2 * 2.303 * A_0 * DF}{C * \varphi * \theta * 1000} \quad (4)$$



where  $A_0$  is the absorbance of diluted emulsion after homogenization,  $DF$  is the dilution factor,  $C$  is the protein concentration,  $\varphi$  is the optical path,  $\theta$  is the oil volume fraction.

The same procedure was repeated at 10 and 30 min and absorbance values were used to determine emulsion stability index (ESI) values. ESI were calculated according to the following equation (Eq. (5)).

$$ESI(\text{min}) = \frac{A_0}{(A_0 - A_r)} * t \quad (5)$$

where  $A_0$  is the absorbance of diluted emulsion after homogenization,  $A_r$  is the absorbance of diluted emulsion at related time (at 10 or 30 min) [21].

### Stability coefficient

Ten mL samples were taken from emulsions and centrifuged for 15 min at 2000 rpm. After centrifugation, liquid phase was diluted 100 times. Absorbance of the diluted and original samples was read at 750 nm and noted. Stability coefficient was calculated according to the following equation (Eq. (6)).

$$\text{Stability coefficient}(R) = \frac{A_d}{A_o} * 100 \quad (6)$$

where  $A_o$  is the absorbance of original samples and  $A_d$  is the absorbance of diluted supernatant [22].

### Centrifugal precipitation rate

Centrifugal precipitation rate (CPR) was determined according to the method of Li et al. [22]. Briefly, 10 mL emulsion was transferred to a centrifuge tube. After samples were centrifuged at 2500 rpm for 40 min, liquid phase was removed. Centrifuge tubes were kept inverted for 30 min. Then, amount of residue (% w/w) was determined. Centrifugal precipitation rate was calculated by the following equation (Eq. (7)).

$$CPR(\%) = \frac{W_2}{W_1} * 100 \quad (7)$$

where  $W_1$  is the weight of emulsion,  $W_2$  is the weight of precipitation after centrifugation.

### Stability index

Ten mL emulsion was added to a 15 mL centrifuge tube. Samples were centrifuged at 4000 rpm for 5 min. Volume ratios of upper phase (oil), middle phase (emulsion) and lower phase (serum) were measured and noted to comment stability index [23].

## Emulsion stability under stress conditions

To determine the stability of emulsions against pH, their pH was adjusted (1 M NaOH or 1 M HCl) to different levels (3.0, 5.0, 7.0, 9.0, and 11.0) by stirring for 1 h. To assess resistance to ionic stress, different concentrations (0–500 mM) of salt (NaCl) were added to emulsions. It was vortexed at room temperature for 1 min and kept for 15 min. To evaluate thermal stability of emulsions, they were heated at 20, 40, 60, 80, and 100 °C for 30 min. Next, samples were brought to room temperature and stored for 24 h [24]. For freeze-thawing, samples at pH 7.0 were kept at -18 °C for 72 h and then thawed at room temperature for 2 h [25]. Emulsion images and particle size changes were detected.

## Optical microscopy and particle size analyses

An optical microscope with objective lens (10× and 40×) was used to detect droplet size differences between emulsions. One drop was taken from each sample, placed on the slide, and images were taken by placing a coverslip on it [26]. Droplet size was calculated by ImageJ program and results were presented as mean diameters.

## Statistical analysis

All analyses were performed in three replications. Mean values, standard deviations and all plots were obtained with OriginPro 2021b (Origin Lab Inc.). The obtained data were performed with SPSS 22 (SPSS Inc., Chicago, IL, USA) statistical package for Windows using independent samples t-test ( $p < 0.05$ ) or One-way ANOVA (Tukey's HSD).

## Results and discussion

### Browning intensity

Browning intensity value is an indicator to put forth the Maillard conjugation degree [9]. Therefore, knowing this value is one of the most fundamental for determining the suitability of carbohydrates used in conjugating proteins. In this context, browning intensity of samples was investigated spectroscopically in the present study and results are shown in Fig. 2A. As expected, superior browning intensity was detected in conjugates compared to SCPI alone but intensity value differed according to carbohydrate type preferred in the system where the process is carried out. Conjugation degree was higher in SCPI-P (0.593) followed by SCPI-CMC (0.534) and SCPI-GA (0.352). Pectin is a convenient polysaccharide for conjugation as it possesses more reducing ends and is less steric [27]. Another comment regarding carbohydrate behaviors in the Maillard reaction, they exhibit a

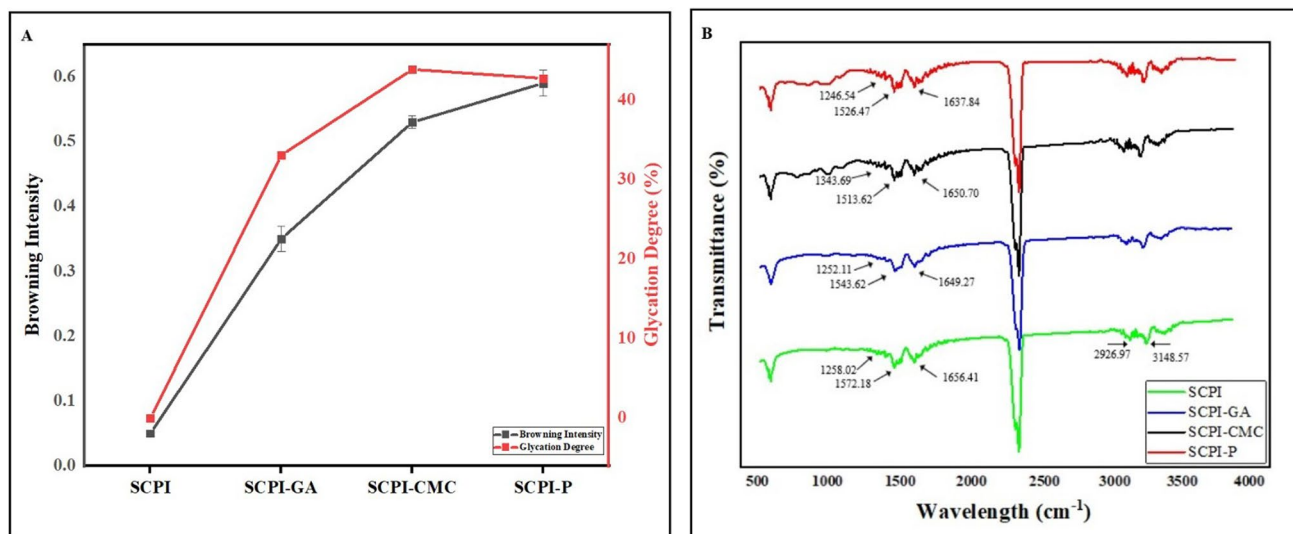


**Fig. 2** Browning intensity and glycation degree (A) and FTIR spectrum (B) of sour cherry seed protein isolate (SCPI), sour cherry seed protein isolate-gum Arabic conjugate (SCPI-GA), sour cherry seed protein isolate-carboxymethyl cellulose (SCPI-CMC) and sour cherry seed protein isolate-pectin conjugate (SCPI-P)

similar mechanism during the first stage of conjugation [28]. Eminent reaction observed in the presence of P and CMC may have occurred at the last phase of the Maillard conjugation. It can be said that there is an intense binding between proteins and these carbohydrates in this phase, and thus the changes in the fractional conformation of proteins are more comprehensive compared to GA ones [29].

### Glycation degree

Another indicator to evaluate processes of the Maillard conjugation is the glycation degree. A positive correlation was reported between these two parameters in the previous study [30]. Free amino group of protein and the carbonyl group of the reducing sugar react during the conjugation. This carbonyl ammonia condensation reaction results in the reduction of free amino group in protein [31]. Based on this approach, glycation degree is defined by establishing the changes in free amino group content of proteins [31, 32]. Figure 2A shows the glycation degree of samples. Carbohydrate type possessed a significant effect on glycation degree (33.07% for SCPI-GA, 43.86% for SCPI-CMC, and 42.73% for, SCPI-P). This trend was also supported by browning intensity values and amino acid distribution results. For this reason, a similar interpretation as that of browning intensity could be noted here as well to explain notable differences. Reason for superior glycation degree in the SCPI-CMC and SCPI-P could be associated with the special structure (more reducing ends and less steric) of CMC and P. As for the SCPI-GA, undesirable glycation degree compared to

protein isolate-carboxymethyl cellulose (SCPI-CMC) and sour cherry seed protein isolate-pectin conjugate (SCPI-P)

the others could be ascribed to a mighty steric obstruction efficacy [31].

### FTIR spectrums

FTIR spectroscopy analysis, as a vibrational spectrum, is a practical method used to understand the interaction of protein-polysaccharide during the Maillard conjugation. Shifts and decreases in FTIR absorption peaks can be observed, and even new absorption peaks can become visible when intermolecular and intramolecular bonds interact [13]. FTIR spectrums of protein and the Maillard conjugates formed with different polysaccharides are presented in Fig. 2B. Amide A and amide B signals associated with symmetrical stretching of C–H and NH<sub>2</sub> in SCPI were observed in the wavelengths of 3148.57 and 2926.97 cm<sup>-1</sup>, respectively. Peaks related to these specific groups were also detected in conjugate spectrums but their intensity/broadness was grander than that of protein ones. As a result of the Maillard reaction between proteins and polysaccharides, changes may occur in these regions where free –OH and –NH<sub>2</sub> are in FTIR spectra. These phenomena could be ascribed to covalent bonds between carbonyl groups in saccharides and amino groups in protein bonds as a natural consequence of process. Thus, hydroxyl group at the end of the sugar ring decays and this situation causes vibration in FTIR spectra [33]. Amide-I (C=O stretching), amide-II (N–H deformation) and amide-III (C–N stretching and N–H deformation) bands, known as fingerprint region of proteins, are located in the wavelength of 1700–1600 cm<sup>-1</sup>, 1550–1500 cm<sup>-1</sup> and 1300–1200 cm<sup>-1</sup>, respectively [10]. Absorption peaks were

detected in these regions for all samples, namely proteins and conjugates. These peaks in SCPI were in the 1258.02, 1572.18, and 1656.41  $\text{cm}^{-1}$  representing amide I, amide II, and amide III, respectively. On the other hand, these protein-specific structures were seen at lower wavelengths in conjugates (amide I: 1252.11  $\text{cm}^{-1}$  (SCPI-GA), 1343.69  $\text{cm}^{-1}$  (SCPI-CMC), and 1246.54  $\text{cm}^{-1}$  (SCPI-P); amide II: 1543.62  $\text{cm}^{-1}$  (SCPI-GA), 1513.62  $\text{cm}^{-1}$  (SCPI-CMC), and 1526.47  $\text{cm}^{-1}$  (SCPI-P); amide III: 1649.27  $\text{cm}^{-1}$  (SCPI-GA), 1650.70  $\text{cm}^{-1}$  (SCPI-CMC), and 1637.84  $\text{cm}^{-1}$  (SCPI-P)). This phenomenon could be attributed to reduction of  $-\text{NH}_3$  during the Maillard reaction [34]. Considering the changes in FTIR spectra, it could be said that proteins were successfully bound to proper places of carbohydrates.

As for variation among conjugates, more intensity/broadness and shifts were determined in spectrums of conjugates obtained in the presence of P and CMC compared to SCPI-GA. This means that P and CMC as the carbohydrate side of the Maillard conjugation are in the foreground compared to GA. This phenomenon was in accordance with the results of browning intensity and glycation degree.

## Amino acid content

Amino acid fractions of SCPI were investigated by LC-MS/MS before and after glycation in this part. The  $\epsilon$ -amino groups of proteins and the reducing-end carbonyl groups of carbohydrates are responsible for covalent binding occurring the related process. Major locations from protein side are associated with  $\epsilon$ -amino groups of lysine and arginine [35]. Graft reactions result in the decrease of these two amino acids [36]. These previous phenomena were supported by the findings obtained in the current study. Superior lysine level was detected in SCPI (6.79%) followed by SCPI-GA (5.80%), SCPI-P (2.78%), and SCPI-CMC (2.69%). Similar trend was observed for arginine content and ratio of this amino acid was found as 7.32, 5.10, 3.68, and 3.53% for SCPI, SCPI-GA, SCPI-P, and SCPI-CMC, respectively (Table 1). Levels of decline in the lysine and arginine depending on carbohydrate type were in line with browning intensity and glycation degree. Quantitative shift level of lysine in proteins after the Maillard reaction provides information about glycation degree [37].

## Scanning electron microscopy (SEM)

Morphological properties of protein and conjugates were examined by SEM and micrographs are shown in Fig. 3A. SCPI possessed a non-uniform structure and indistinguishable surface conformation. Similar surface morphology for plant-based proteins was explained in previous research [10]. Visible differences were detected differences in the natural appearance of protein after conjugation process. Rough

**Table 1** Amino acid contents of protein isolate and Maillard conjugates

Amino acids	Content (%)			
	SCPI	SCPI-GA	SCPI-CMC	SCPI-P
<b>Essential amino acids</b>				
Histidine	2.39	2.62	2.81	3.40
Leucine	6.88	6.13	7.07	7.06
Isoleucine	5.38	5.15	5.54	5.34
Lysine	6.79	5.80	2.69	2.78
Methionine	0.59	0.34	0.81	0.73
Phenylalanine	3.37	4.51	4.87	4.72
Threonine	3.27	2.94	3.21	3.03
Tryptophan	0.00	0.00	0.01	0.00
Valine	3.48	5.80	6.80	6.57
Total	32.15	33.29	33.81	33.63
<b>Non-essential amino acids</b>				
Alanine	6.70	5.84	5.68	5.64
Arginine	7.32	5.10	3.53	3.68
Asparagine	0.00	0.00	0.07	0.03
Aspartic acid	9.25	10.57	11.06	9.93
Citrulline	0.48	0.44	0.46	0.56
Glutamine	0.03	0.02	0.01	0.01
Glutamic acid	16.02	18.28	18.14	18.10
Glycine	8.56	7.93	9.55	9.48
Alloisoleucine	0.03	0.03	0.03	0.03
Ornithine	0.06	0.07	0.13	0.58
Proline	5.62	5.52	5.22	5.70
Serine	5.62	5.64	5.06	5.27
Tyrosine	2.21	1.74	2.92	2.61
Alphaaminoadipic acid	0.00	0.01	0.01	0.01
Alphaaminopimelic acid	0.01	0.04	0.05	0.04
Anserine	0.11	0.28	0.36	0.47
Argininosuccinic acid	0.00	0.00	0.00	0.00
Alphaaminobutyric acid	0.06	0.06	0.04	0.05
Betaaminoisobutyric acid	0.36	0.32	0.24	0.25
Gammaminobutyric acid	1.59	1.40	1.35	1.29
Beta-alanine	0.13	0.11	0.09	0.09
Sarcosine	0.58	0.51	0.49	0.52
Cystathionine	0.00	0.00	0.00	0.00
Thiaproline	0.01	0.01	0.00	0.00
1-Methylhistidine	0.00	0.00	0.00	0.00
3-Methylhistidine	0.00	0.00	0.00	0.00
Hydroxylysine	0.00	0.00	0.00	0.00
Hydroxyproline	2.71	2.41	2.18	2.32
Cystine	0.33	0.32	0.38	0.32
Homocystine	0.00	0.00	0.00	0.00
Serotonin	0.00	0.00	0.00	0.00
Histamine	0.00	0.00	0.00	0.00
Etanolamine	0.03	0.08	0.03	0.08
Phosphoethanolamine	0.00	0.00	0.00	0.00
5-Oh-Trp	0.00	0.00	0.00	0.00
Taurine	0.00	0.00	0.00	0.00
Total	67.82	66.73	67.08	67.06

SCPI-GA Sour cherry seed protein isolate-gum Arabic conjugate, SCPI-CMC Sour cherry seed protein isolate-carboxymethyl cellulose conjugate, SCPI-P Sour cherry seed protein isolate-pectin conjugate

structures predominated in the conjugates. Micrograph of GA-conjugate showed half spirals and inhomogeneous overlapping sheets. Conjugates containing P displayed irregular sheet structure and intermittent network structure. In addition, covalent bonds formed between SCPI and CMC via the Maillard reaction resulted in an intense composite network structure and smoother surface. In a study on the Maillard conjugates, it was reported that morphological structures of final products differ according to the materials preferred in conjugation [38]. Results of another study also support this approach [10]. Reason for the structural diversity among the conjugates could be related to the interaction level between the chosen polysaccharides and the protein [39]. When the term, interaction level, was elaborated, each polysaccharide contains independently different amounts of various reducing sugars (glycosyl groups). More protein molecules could bind or access to polysaccharide containing more glycosyl groups, leading to predominance of compact structures in morphological images. Presumably, the situation in conjugate (SCPI-CMC) having more compact structure might be ascribed to the mentioned phenomenon. Similar approaches were noted in elsewhere [32, 40]. Browning intensity and glycation degree values were in line with these comments. Also, the mentioned approaches were supported by findings reported for FTIR spectra. The most spectrum shift and peak depth changes causing intense intramolecular glycation were detected in conjugates containing CMC and P. Probably, intense intramolecular glycation may be the reason for the rigid layer structure in SEM images of SCPI-CMC. These

values clearly indicated that interaction level was not equal for conjugates.

### Thermal gravimetric analysis (TGA)

TGA analysis was performed to detect weight loss of protein and conjugates against thermal degradation. As presented in Fig. 3B, weight loss (%) of samples occurred in 3 stages between 30 °C and 1000 °C. Initial weight losses (about 9%) of all samples occurred below 180 °C. This phenomenon might be attributed to evaporation of free and bound water in samples [18]. The biggest event happened in second step at temperature of 250–450 °C for protein and conjugates while their weight loss levels were not equal. In this step, maximum weight loss was detected in SCPI (59.86%) followed by SCPI-GA (36.34%), SCPI-CMC (28.91%) and SCPI-P (35.22%). Lower weight loss in the Maillard conjugates was associated with more or different bonds between protein and different polysaccharides during the Maillard reaction [41]. These cases were also supported by FTIR spectra of proteins and conjugates. The -NH<sub>3</sub> groups in proteins were reduced by the Maillard reaction. Therefore, shifts/intensity or broadness occur in C=O stretching (Amide-I), N-H deformation (Amide-II) and C-N stretching/N-H deformation (Amide-III) bands in conjugates [10]. This was attributed to the strong covalent bond formation between aldehyde groups in polysaccharides and amino groups in proteins polymerized during the Maillard reaction [34]. In the second step of the TGA analysis, the newly formed covalent bonds are

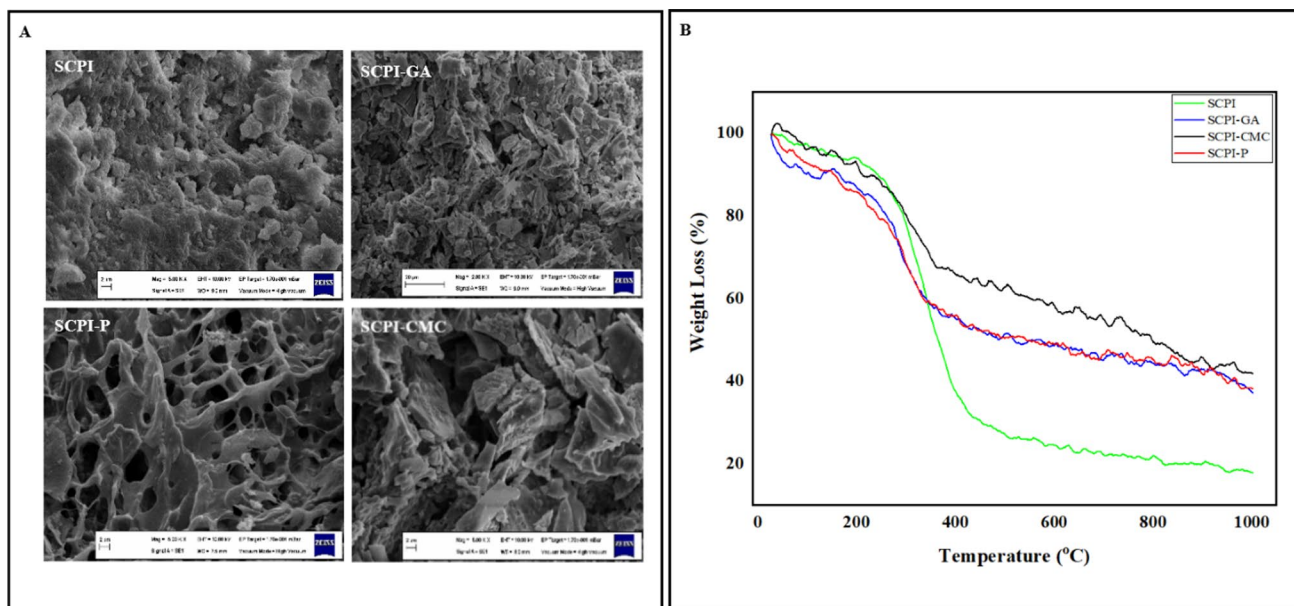


**Fig. 3** Scanning electron microscopy images (A) and the effect of Maillard conjugation on thermal behavior (B) of sour cherry seed protein isolate and Maillard conjugates. SCPI-GA: Sour cherry seed

protein isolate-gum Arabic conjugate, SCPI-CMC: Sour cherry seed protein isolate-carboxymethyl cellulose conjugate, SCPI-P: Sour cherry seed protein isolate-pectin conjugate



more robust to temperature and the mass loss is less in the conjugates. Protein not included in the Maillard conjugation lost all of its mass at the end of the third step. Unlike this situation, samples prepared in the presence of GA, CMC, and P largely retained their mass (approximately 50%). High levels of mass residues in conjugates might be associated with the reaction of polysaccharides with some groups in the proteins and formation of cross-links in protein–protein interactions [10].

## Functional properties

Functional properties (solubility, water holding capacity, oil holding capacity, foaming capacity, foaming stability, emulsion activity, and emulsion stability) of samples are presented in Table 2. Solubility is a one of the most fundamental functional attributes of proteins that possesses impacts on other techno-functional behaviors. Polysaccharide type possessed a significant effect on solubility (77.17% for SCPI-GA, 82.68% for SCPI-CMC, and 80.81% for SCPI-P). Protein-polysaccharide interactions were found to statistically effective on solubility ( $p < 0.05$ ). This trend was also supported by other functional properties values. SCPI-CMC and SCPI-P conjugates displayed superior solubility than that of SCPI-GA conjugate. Protein-polysaccharide conjugates have more hydrophilic groups than protein alone. In studies on Maillard conjugates, it was reported that interaction with anionic polysaccharides such as P and CMC increases negative charges on protein surface and possess an important share in improving solubility [42, 43].

Water holding capacity of SCPI was found as 242.91%. Alterations in chemical conformation of materials may remarkably change their water holding capacity [44]. This approach was supported in the present study. Water holding capacity was not detected in conjugates as they were exactly dissolved in aqueous phase. This value varies may not be

calculated in fully soluble materials [10]. As for oil holding capacity, the Maillard-derived conjugates formed with 3 different polysaccharides (GA, CMC, and P) displayed superior capacity in terms of oil holding compared to protein alone (228.09%). SCPI-CMC possessed maximum oil holding capacity (569.09%) followed by SCPI-P (535.24%) and SCPI-GA (503.51%). The Maillard-derived conjugates own greater oil holding capacity than that of protein alone [10]. Development of oil holding capacity is related to hydrophobic groups on surface of protein molecule [45]. Correlation between glycation degree and hydrophobic groups was reported by a previous study [46]. With increase of glycation degree, the distortions in hydrophobicity-hydrophilicity balance increase, resulting in enhancing hydrophilicity (oil holding capacity) of final products [47]. When examined glycation degree values and FTIR spectrums, the changes in hydrophobicity-hydrophilicity balance were higher in SCPI-CMC followed by SCPI-P and SCPI-GA. The level of these changes was closely related with oil holding capacity findings. As mentioned in SEM section, the amount of reducing sugars (glycosyl groups) could be responsible for these results. Ultimately, the desired increase in terms of this functional attribute could be ascribed to the emergence of hydrophobic residues of SCPI during covalent binding of polysaccharide to the protein. This comment was in line with a previous study [48].

Foaming capacity and stability of samples are presented in Table 2. Interactions and molecular changes after the Maillard reaction played a role in enhancing foam behavior of SCPI. Foaming capacity of protein alone was 60.00%. Polysaccharide type possessed a significant effect on foaming capacity (70.00% for SCPI-GA, 80.00% for SCPI-CMC, and 79.00% for SCPI-P). Protein-polysaccharide interactions were found to statistically effective on foaming capacity ( $p < 0.05$ ). Also, SCPI exhibited superior foaming stability than that of conjugates ( $p < 0.05$ ).

**Table 2** The effect of Maillard conjugation on functional properties of protein isolate

	SCPI	SCPI-GA	SCPI-CMC	SCPI-P
Solubility	68.26 ± 0.65 <sup>c</sup>	77.17 ± 2.28 <sup>b</sup>	82.68 ± 3.26 <sup>a</sup>	80.81 ± 1.31 <sup>ab</sup>
Water holding capacity (%)	242.91 ± 3.98	nd	nd	nd
Oil holding capacity (%)	228.09 ± 1.02 <sup>d</sup>	503.51 ± 1.10 <sup>c</sup>	569.09 ± 1.69 <sup>a</sup>	535.24 ± 1.87 <sup>b</sup>
Foaming capacity (%)	60.00 ± 2.83 <sup>b</sup>	70.00 ± 2.83 <sup>ab</sup>	80.00 ± 2.83 <sup>a</sup>	79.00 ± 1.41 <sup>a</sup>
Foaming stability (%)	59.96 ± 1.89 <sup>c</sup>	85.70 ± 0.58 <sup>b</sup>	96.21 ± 1.90 <sup>a</sup>	91.12 ± 1.95 <sup>ab</sup>
Emulsion activity EAI (m <sup>2</sup> /g)	7.00 ± 0.91 <sup>c</sup>	14.29 ± 0.09 <sup>b</sup>	16.41 ± 0.10 <sup>ab</sup>	18.66 ± 1.07 <sup>a</sup>
Emulsion stability (ESI10) (min)	45.49 ± 0.92 <sup>c</sup>	62.20 ± 0.62 <sup>b</sup>	72.74 ± 0.05 <sup>a</sup>	73.65 ± 0.81 <sup>a</sup>
Emulsion stability (ESI30) (min)	41.93 ± 1.95 <sup>c</sup>	54.31 ± 1.33 <sup>b</sup>	57.93 ± 0.82 <sup>ab</sup>	62.59 ± 0.76 <sup>a</sup>

SCPI-GA Sour cherry seed protein isolate-gum Arabic conjugate, SCPI-CMC Sour cherry seed protein isolate-carboxymethyl cellulose conjugate, SCPI-P Sour cherry seed protein isolate-pectin conjugate

Data are expressed as a mean ± standard deviation of three replicate (n=3). Results were expressed as mean ± standard deviation. Statistical differences were presented by dissimilar letters in the same graph among the samples ( $p < 0.05$ )

SCPI-CMC conjugate showed the highest stability (96.21%). In a study, it was noted that positive effects were observed on foaming properties of protein-polysaccharide complexes [49]. Like oil holding capacity and emulsion behavior, this phenomenon could be because of hydrophobic parts of protein. Foam properties of proteins bound up with their talent to diffuse to air–water interface, adsorb to interface, and realign or undergo conformational alterations at interface to lower surface tension. Partially untied protein structure to uncover hydrophobic parts encourage greater interactions on air–water interface. Joining of polysaccharides and the ensuing formation of complexes contribute to foaming stability through improved absorption at interface and creation of a viscoelastic film between neighboring air bubbles [11].

EAI and ESI are parameters used to determine emulsifying properties of proteins. EAI was  $7.00 \text{ m}^2/\text{g}$  for SCPI. This value was significantly advanced after the Maillard reaction and found as  $14.29 \text{ m}^2/\text{g}$  for SCPI-GA,  $16.41 \text{ m}^2/\text{g}$  for SCPI-CMC, and  $18.66 \text{ m}^2/\text{g}$  for SCPI-P (Table 2). Considering ESI, it was observed that emulsions formed with conjugates preserved their stability more than that of protein alone. These findings were supported by oil holding capacity results and previous studies. Emulsifier behavior of proteins in oil-in-water emulsions could be enhanced by the Maillard conjugation process [50]. However, the current study results indicated that it was not possible to get the same effect in all carbohydrates and the selected carbohydrates type for complexes possessed remarkable efficacy on interfacial functionality of proteins. EAI and ESI of the Maillard-based conjugates depend on the carbohydrate side of covalent combination [51–55].

### Stability coefficient, centrifugal precipitation rate, and stability index

R and CPR of emulsions stabilized by SCPI and the Maillard conjugates are given in Fig. 4A. There is a positive correlation between R and emulsion stability. Conjugation process owned a notable effect on R value. This value showed an increasing trend with utilization of the Maillard conjugates as emulsifier in emulsion preparation. R was 0.60 for SCPI emulsion and 0.87, 0.94 and 0.95 for SCPI-GA, SCPI-CMC, and SCPI-P emulsions, respectively. Datasets indicated that conjugates displayed superior surface-active attribute. This situation could be explained by the increasing electrostatic repulsion forces, deactivating flocculation creation in the presence of carbohydrates. Herewith, particles remain suspended in the emulsion, providing higher emulsion behavior [22].

In contrast to R, CPR is a negative marker of emulsion stability. Addition of conjugates to emulsions resulted in a lower centrifugal precipitation rate compared to SCPI emulsions, as seen in Fig. 4A. While the CPR was 59.17% in the presence of SCPI, this value decreased to 36.04%, 32.61%, and 30.92% with the addition of SCPI-GA, SCPI-CMC, and SCPI-P to emulsions, respectively. These phenomena might be ascribed to the desired oil droplet absorption capacity of SCPI-P and SCPI-CMC compared to those of SCPI alone and SCPI-GA [56]. A previous study revealed that addition of carbohydrate to rapeseed protein isolate at pH 7.0 significantly reduces CPR of emulsion [22]).

Stability index of emulsions is shown in Fig. 4B. It was investigated according to the post-centrifuge phase separation images of emulsions formed from protein and

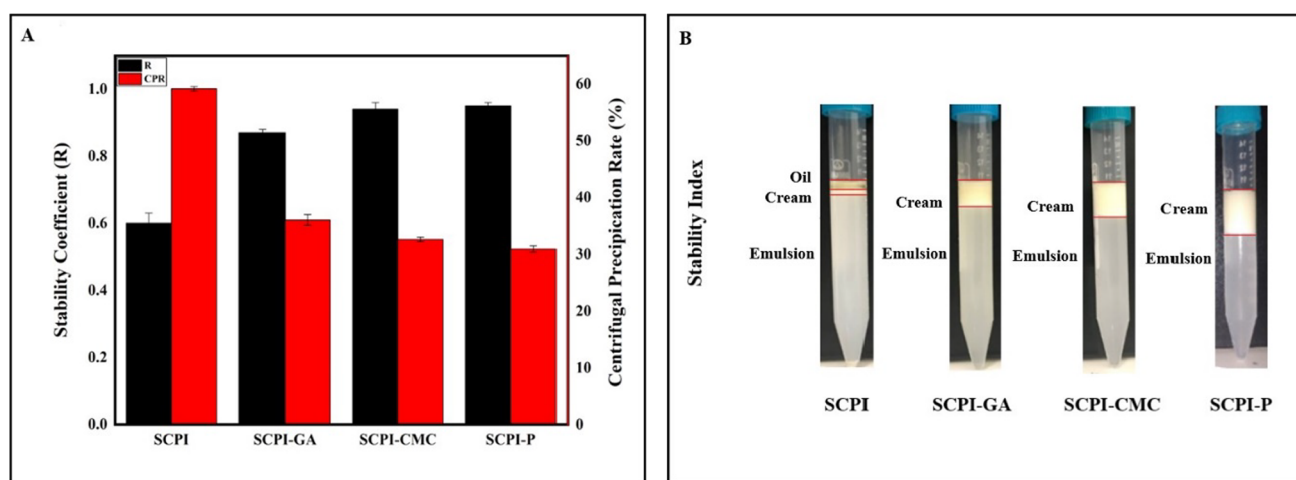


**Fig. 4** Stability coefficient and centrifugal precipitation rate (A) and stability index results (B) commented according to visuals of the emulsion layers of sour cherry seed protein isolate (SCPI) and Maillard conjugates emulsions. SCPI-GA: Sour cherry seed protein

isolate-gum Arabic conjugate, SCPI-CMC: Sour cherry seed protein isolate-carboxymethyl cellulose conjugate, SCPI-P: Sour cherry seed protein isolate-pectin conjugate

conjugates. Stability index was observed that emulsion formed with protein alone was divided into three phases as oil phase (upper phase), cream (middle phase), and emulsion (lower phase) while no oil phase separation was observed in emulsions formed with conjugates (Fig. 4B). These separation levels, most notably oil and serum layer, are the factors used to put forth emulsion stability and these levels varied in emulsions formed with SCPI and its conjugates [57]. Emulsions formed with conjugates are more stable; indicating that coupling of conjugates with SCPI via the Maillard reaction can be an influential application for significantly developing the surfactant property of the protein.

## Emulsion stability under stress conditions

### Freeze-thawing

In this part, stability properties of freeze-thawed emulsions were investigated. For this, emulsions were frozen at  $-18\text{ }^{\circ}\text{C}$  for 72 h and then thawed for 2 h at  $24\text{ }^{\circ}\text{C}$ . Droplet sizes, images, and light microscope appearances of fresh and thawed emulsions were examined (Figs. 5A, B, C). An increase was found in mean droplet diameter of freeze-thawed emulsions at the end of the treatment compared to freshly prepared ones. Mean diameter in fresh emulsions containing SCPI alone, SCPI-GA, SCPI-CMC, and SCPI-P was 20.73, 15.67, 10.36, and 12.64  $\mu\text{m}$ , respectively while these values reached to 35.61, 25.17, 19.11, and 22.61  $\mu\text{m}$  after freeze-thawed proses (Fig. 5A). Minimum particle size

represents superior stability in emulsions prepared by using conjugates [58]. This approach was supported by images and light microscope appearances of emulsions. Two phases including cream and emulsion with spread minor oil droplets were observed in all fresh emulsions (Fig. 5B). Emulsions formed in the presence of SCPI-P and SCPI-CMC kept their stability after freeze–thaw cycle. However, a third phase, namely oil was seen in emulsions stabilized by using SCPI alone and SCPI-GA. Oil phase level in emulsions used SCPI alone was too obvious than that of SCPI-GA ones. Moreover, a visible serum layer was detected in SCPI emulsions but no other ones. Results clearly showed that resistance of emulsions prepared by using protein alone against freeze-thawed was lower than those of emulsions containing conjugates, especially SCPI-P and SCPI-CMC. It is more reasonable to use conjugates as an emulsifier for forming more stable emulsions against freeze-thawed rather than protein alone [25, 59]. The Maillard conjugates provide formation of a thicker interfacial stratum in oil-in-water emulsions. This situation prevents the aggregation of oil droplets and thus more stable emulsions are formed [60].

### Ionic stress

Salt, a universal spice in foods, not only reduces surface potential of colloidal particles but can also cause them to coagulate/flocculate [23]. At this stage of the study, stability behavior of emulsions prepared using SCPI and conjugates against ionic strength (0–500 mM NaCl) was evaluated.

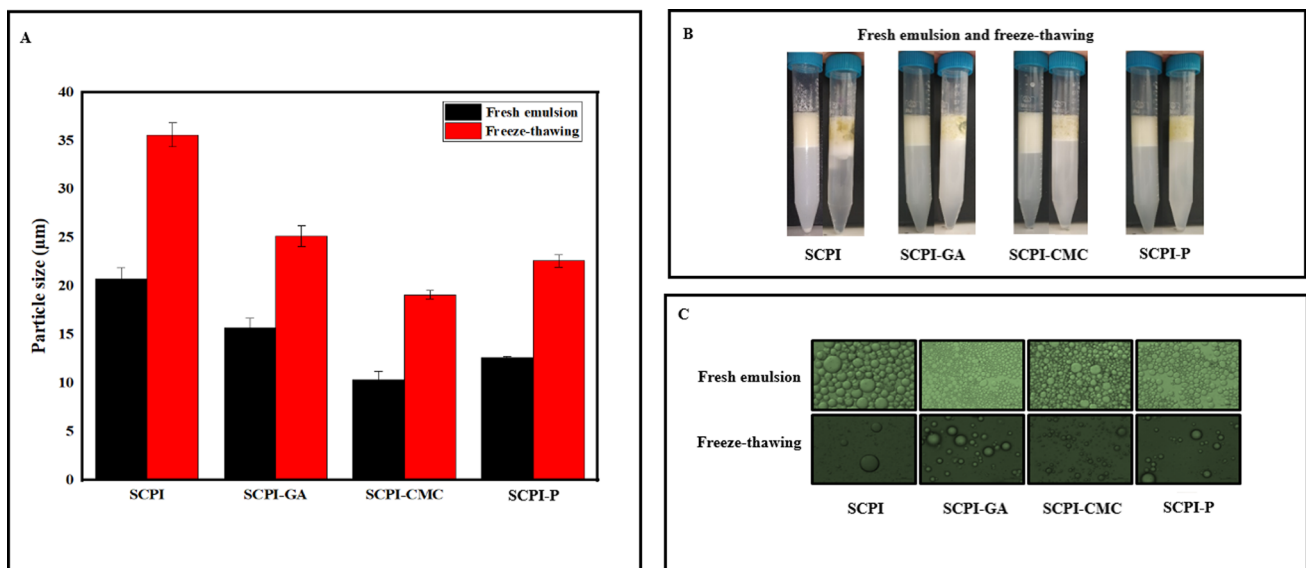


**Fig. 5** Particle size before and after freeze–thaw treatment (A) of sour cherry seed protein isolate (SCPI) and Maillard conjugates emulsions, appearances (B), and microscopic observations (C) of the emulsions. Data are expressed as a mean  $\pm$  standard deviation of

three replicate ( $n=3$ ). SCPI-GA: Sour cherry seed protein isolate-gum Arabic conjugate, SCPI-CMC: Sour cherry seed protein isolate-carboxymethyl cellulose conjugate, SCPI-P: Sour cherry seed protein isolate-pectin conjugate

This behavior was commented by using different parameters, namely mean droplet diameter, emulsion images, and light microscope appearances (Figs. 6A, B, C). A gradual increase in particle size of all emulsions was detected with increasing salt concentration from 0 to 500 mM. At the lowest NaCl concentration, mean droplet diameter was 38.34, 11.50, 10.69, and 7.90 for emulsions formed with SCPI alone, SCPI-GA, SCPI-CMC, and SCPI-P, respectively while it was measured as 54.66, 27.74, 21.37, and 14.20 at the highest concentration. Lower particle size, a remarkable indicator for stability, was established in conjugate emulsions. Emulsions stabilized in the presence of SCPI-P and SCPI-CMC showed the most resistance against ionic stress. This phenomenon could be because of stronger bonds (van der Waals, hygroscopic, etc.) formed between SCPI and the related carbohydrates during the Maillard reaction. Strength of pectin as a protein-supporting material in emulsion systems was confirmed in a previous study [24]. Success of SCPI-P and SCPI-CMC was also supported by emulsion images and light microscope appearances. In emulsions formed with SCPI alone, a remarkable differentiation in images and oil phase separation was observed with increasing salt concentrations (Fig. 6B). However, no distinguishable oil separation was detected in conjugate emulsions, especially SCPI-P and SCPI-CMC. This means that conjugates possessed a power to prevent oils aggregation although the force of attraction between droplets increased depending on the salt concentration. Also, this power was

seen in light microscope appearances. Oil droplets in SCPI emulsions tended to be more aggregate compared to others.

### pH-shifting

In this study, resistance of emulsions to pH change was evaluated according to mean droplet diameter, emulsion images, and light microscope appearances (Figs. 7A, B, C). As shown in Fig. 7A, mean droplet diameters of emulsions stabilized using protein alone were higher than droplet diameters of emulsions formed in the presence of conjugates at all pHs. Particle size at pH 3.0, 5.0, 7.0, 9.0, and 11.0 was 28.21, 33.27, 19.90, 28.40, and 42.32  $\mu\text{m}$  for SCPI alone, 18.67, 23.84, 15.77, 21.10, and 29.49  $\mu\text{m}$  for SCPI-GA, 13.15, 14.28, 10.69, 16.73, and 20.36  $\mu\text{m}$  for SCPI-CMC and 17.69, 15.05, 12.14, 17.81, and 22.27  $\mu\text{m}$  for SCPI-P, respectively. According to the results of droplet sizes, sample having less resistance to creaming and agglomeration was emulsion prepared with SCPI alone, followed by SCPI-GA, SCPI-P, and SCPI-CMC ones. These results were in line with emulsion images and light microscope appearances. When Fig. 7B is examined, oil separation was detected only in samples prepared with protein alone at pH 11. In addition, serum formation was observed in all samples except for SCPI-CMC emulsions at low pHs. Reason for serum layer at low pH could be attributed to the decrease in the electrostatic repulsion force because of the proximity to isoelectric point of proteins [24]. SCPI-CMC conjugates

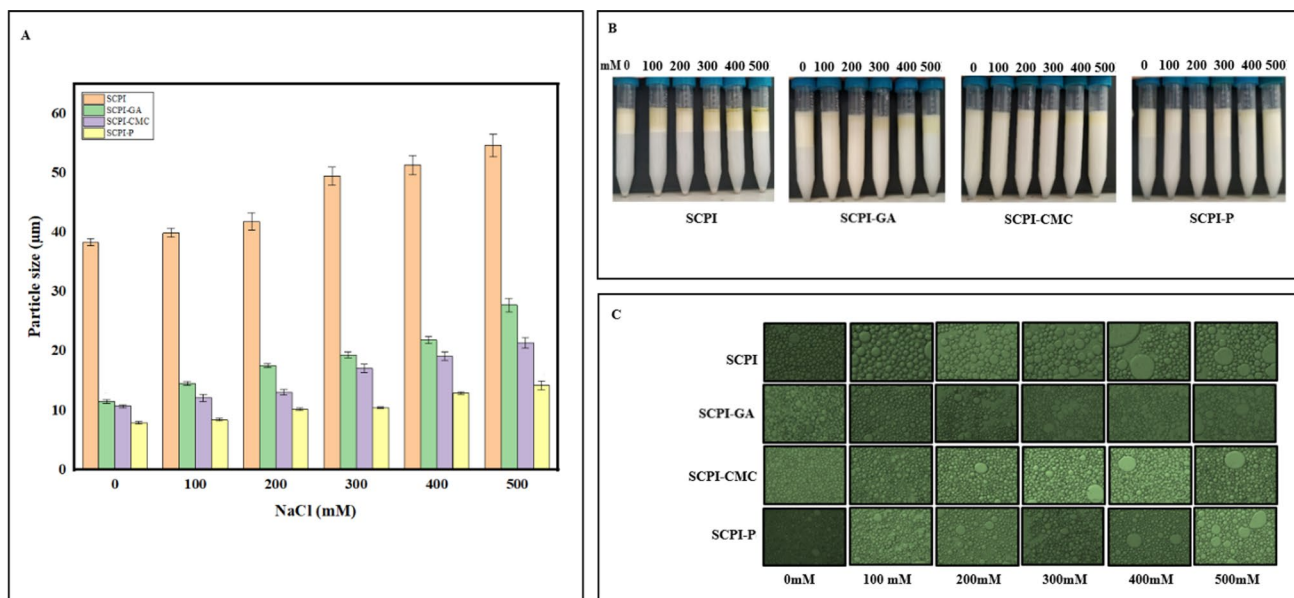


**Fig. 6** Ionic stability of sour cherry seed protein isolate (SCPI) and Maillard conjugates emulsions. Particle sizes (A), appearances (B), and microscopic observations of the emulsions (C). Data are expressed as a mean  $\pm$  standard deviation of three replicate ( $n=3$ ).

SCPI-GA: Sour cherry seed protein isolate-gum Arabic conjugate, SCPI-CMC: Sour cherry seed protein isolate-carboxymethyl cellulose conjugate, SCPI-P: Sour cherry seed protein isolate-pectin conjugate



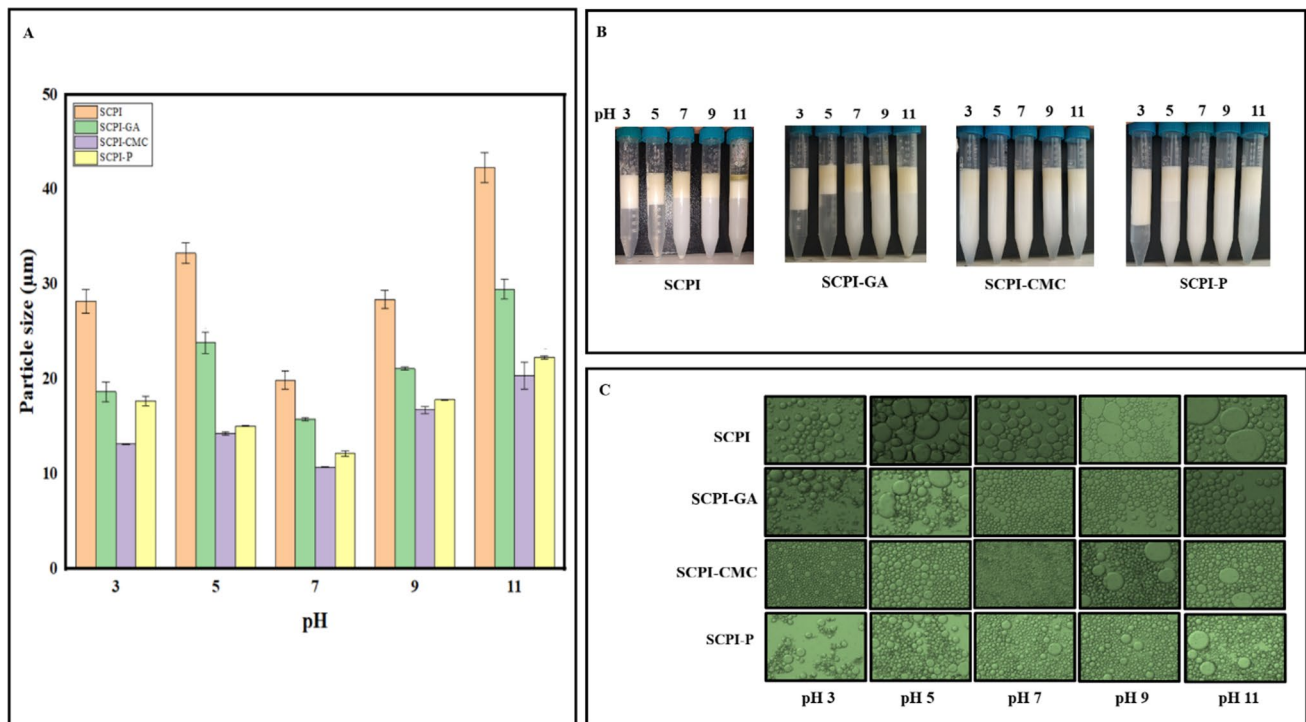


**Fig. 7** pH-shifting stability of sour cherry seed protein isolate (SCPI) and Maillard conjugates emulsions. Particle sizes (A), appearances (B), and microscopic observations of the emulsions (C). Data are expressed as a mean  $\pm$  standard deviation of three replicate ( $n=3$ ).

obstructed serum formation in emulsions at all pHs; indicating that emulsions prepared using them displayed greater resistance to pH-shifting than other polysaccharide-containing emulsions. SCPI-CMC conjugates maximized the steric and electrostatic repulsion forces between emulsion drops, creating a thicker interfacial layer compared to other conjugate ones [60].

### Temperature effect

It is desired that food emulsions are resistant to heat treatments during processing, storage, and use [24]. In this context, different temperature treatments (20, 40, 60, 80, and 100 °C) were applied to emulsions formed with protein alone/the Maillard conjugates in this part of the current study and their stability to temperature was investigated. Emulsion properties were appraised according to mean droplet diameter, emulsion images, and light microscope appearances (Figs. 8A, B, C). Droplet diameter for all samples showed a monomodal distribution (Fig. 8A). As the applied temperature increased, significant increments were found in mean droplet diameter of emulsions. SCPI emulsions displayed the lowest stability. Particle size of emulsions varied in the range of 18.90–32.30  $\mu\text{m}$  when temperature increased from 20 °C to 100 °C. Increase of emulsion mean droplet diameter was

SCPI-GA: Sour cherry seed protein isolate-gum Arabic conjugate, SCPI-CMC: Sour cherry seed protein isolate-carboxymethyl cellulose conjugate, SCPI-P: Sour cherry seed protein isolate-pectin conjugate

evident in emulsion images with oil accumulation (Fig. 8B). Also, this formation was easily detected in optical microscope images (Fig. 8C). This phenomenon could be related to protein denaturation at high temperatures as denaturation causes oil accumulation due to the reduction of interface layer in emulsions. On the other hand, when the Maillard conjugate emulsions were compared with each other, SCPI-P emulsions showed more resistance to thermal change. Mean droplet diameter reached from 8.40  $\mu\text{m}$  to 15.30  $\mu\text{m}$  for SCPI-GA and from 6.10  $\mu\text{m}$  to 12.00  $\mu\text{m}$  for SCPI-CMC with increasing temperature degrees (20–100 °C). According to droplet size results, they did not show sufficient stability compared to SCPI-P emulsions although SCPI-GA and SCPI-CMC emulsions were more stable than protein-alone emulsions. It is thought that reason why particle size was higher in emulsions after heat treatment compared to SCPI-P emulsion was hydrophobicity formed at oil-in-water interface was higher and the adsorbed proteins opened up and showed fewer stable properties [10]. Moreover, no significant changes were detected in emulsion appearances with increasing temperature. These results might be due to the steric and electrostatic repulsion force between conjugates-coated emulsion droplets. Considering all the results, the usage of conjugates as emulsifiers instead of protein alone in process required high temperatures is a more plausible approach.

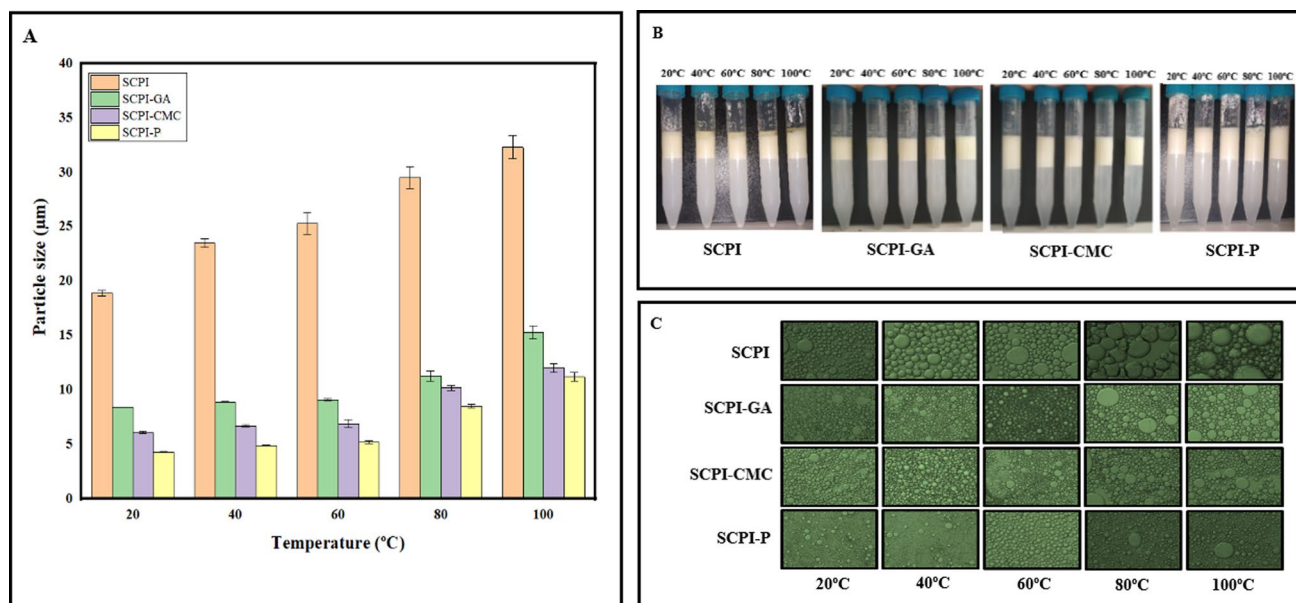


**Fig. 8** Thermal stability of sour cherry seed protein isolate (SCPI) and Maillard conjugates emulsions at different temperatures. Particle sizes (A), appearances (B), and microscopic observations of the emulsions (C). Data are expressed as a mean  $\pm$  standard deviation of

three replicate (n=3). SCPI-GA: Sour cherry seed protein isolate-gum Arabic conjugate, SCPI-CMC: Sour cherry seed protein isolate-carboxymethyl cellulose conjugate, SCPI-P: Sour cherry seed protein isolate-pectin conjugate

## Conclusions

In recent years, the Maillard conjugation system has been widely used for improving surfactant property of plant-based proteins. However, there are numerous options for carbohydrates side of conjugation and the number of studies revealing which carbohydrate is more effective for process is insufficient. Conjugates with the best glycation degree obtained by the Maillard reaction were SCPI-CMC (43.86%), followed by SCPI-P (42.73%) and SCPI-GA (33.07%). EAI values of conjugates (14.29  $m^2/g$  for SCPI-GA, 16.41  $m^2/g$  for SCPI-CMC and 18.66  $m^2/g$  for SCPI-P) were superior than that of protein alone (7.00  $m^2/g$ ). In addition, conjugates especially SCPI-CMC and SCPI-P showed greater resistance to applied environmental stresses (freeze-thawing, ionic stress, pH-shifting, temperature effect). Results highlighted that selection of pectin and/or carboxymethyl cellulose as carbohydrate side of the Maillard conjugation rather than gum Arabic was sensible approximation for enhancing the techno-functional and surfactant attributes of plant-derived proteins. In this context, the data obtained from this study will shed light on future studies. In further studies, conjugates prepared in the current study could be directly evaluated in food systems as emulsifier in food systems including mayonnaise, ice cream, and jelly. Also, they might be evaluated as a coating material in the encapsulation of sensitive core materials namely phenolics and essential oil.

**Acknowledgements** This work was financially supported by Harran University Scientific Research Projects Unit (Project Number: HUBAP-21228). Author Melike YÜCETEPE is supported by the Council of Higher Education (CoHE) with 100/2000 Ph.D. scholarship and Scientific and Technological Research Council of Turkey (TUBITAK; 2211-A) Ph.D. scholarship program.

**Funding** Open access funding provided by the Scientific and Technological Research Council of Türkiye (TÜBİTAK).

## Declarations

**Competing interest** None.

**Open Access** This article is licensed under a Creative Commons Attribution 4.0 International License, which permits use, sharing, adaptation, distribution and reproduction in any medium or format, as long as you give appropriate credit to the original author(s) and the source, provide a link to the Creative Commons licence, and indicate if changes were made. The images or other third party material in this article are included in the article's Creative Commons licence, unless indicated otherwise in a credit line to the material. If material is not included in the article's Creative Commons licence and your intended use is not permitted by statutory regulation or exceeds the permitted use, you will need to obtain permission directly from the copyright holder. To view a copy of this licence, visit <http://creativecommons.org/licenses/by/4.0/>.

## References

1. L. Day, J.A. Cakebread, S.M. Loveday, Trends Food Sci. Technol. **119**, 428 (2022)
2. A.G.A. Sá, Y.M.F. Moreno, B.A.M. Carciofi, Trends Food Sci. Technol. **97**, 170 (2020)

3. M. Kumar, M. Tomar, J. Potkule, Reetu, S. Punia, J. Dhakane-Lad, S. Singh, S. Dhumal, P. Chandra Pradhan, B. Bhushan, T. Anitha, O. Alajil, A. Alhariri, R. Amarowicz, J.F. Kennedy, *Food Hydrocoll* **123**, 106986 (2022)
4. Q. Zhang, Z. Cheng, J. Zhang, M.M. Nasiru, Y. Wang, L. Fu, *J. Food Sci.* **86**, 68 (2021)
5. J. Ding, H. Ju, L. Zhong, L. Qi, N. Sun, S. Lin, *Food Funct.* **12**, 5940 (2021)
6. E. Demirkıran, B. Başıyigit, G. Altun, M. Yüceetepe, H. Sağlam, M. Karaaslan, *Food Hydrocoll.* **133**, 107899 (2022)
7. B. Vani, J.F. Zayas, *J. Food Sci.* **60**, 1025 (1995)
8. F.U. Akharume, R.E. Aluko, A.A. Adedeji, *Compr. Rev. Food Sci. Food Saf.* **20**, 198 (2021)
9. X. Zhang, X. Li, L. Liu, L. Wang, A.F. Massounga Bora, L. Du, *Int. Dairy J.* **102**, 104584 (2020)
10. B. Başıyigit, M. Yüceetepe, G. Akyar, A. Karaaslan, M. Karaaslan, *Colloids Surf. B Biointerfaces* **215**, 112516 (2022)
11. S. Liu, C. Elmer, N.H. Low, M.T. Nickerson, *Food Res. Int.* **43**, 489 (2010)
12. D.J. McClements, S.M. Jafari, *Adv. Colloid Interface Sci.* **251**, 55 (2018)
13. S. Pirestani, A. Nasirpour, J. Keramat, S. Desobry, J. Jasniewski, *Food Hydrocoll.* **79**, 228 (2018)
14. J. Zhang, C. Wen, Y. Duan, H. Zhang, H. Ma, *LWT* **155**, 113004 (2022)
15. S.H.M. Gorissen, J.J.R. Crombag, J.M.G. Senden, W.A.H. Waterval, J. Bierau, L.B. Verdijk, L.J.C. van Loon, *Amino Acids* **50**, 1685 (2018)
16. A. Saglik, I. Koyuncu, A. Gonel, H. Yalcin, F.M. Adibelli, M. Toptan, *Int. Ophthalmol.* **39**, 2325 (2019)
17. B. Başıyigit, A. Görgüç, E. Gençdağ, Ü. Cansu, F. M. Yılmaz, M. Karaaslan, *Biomass Convers. Biorefin.* (2022)
18. B. Başıyigit, M. Yüceetepe, A. Karaaslan, M. Karaaslan, *Mater. Today Commun.* **28**, 102618 (2021)
19. M.M. Bradford, *Anal. Biochem.* **72**, 248 (1976)
20. S.M. Cho, K.S. Kwak, D.C. Park, Y.S. Gu, C.I. Ji, D.H. Jang, Y.B. Lee, S.B. Kim, *Food Hydrocoll.* **18**, 573 (2004)
21. H.W. Lee, Y. Lu, Y. Zhang, C. Fu, D. Huang, *Food Chem.* **358**, 129749 (2021)
22. Q. Li, Z. Wang, C. Dai, Y. Wang, W. Chen, X. Ju, J. Yuan, R. He, *Food Hydrocoll.* **88**, 50 (2019)
23. W. Wang, G. Du, C. Li, H. Zhang, Y. Long, Y. Ni, *Carbohydr. Polym.* **151**, 1 (2016)
24. X. Xu, L. Luo, C. Liu, D.J. McClements, *Food Hydrocoll.* **64**, 112 (2017)
25. D.M. Cabezas, G.N. Pascual, J.R. Wagner, G.G. Palazolo, *Food Hydrocoll.* **95**, 445 (2019)
26. L. Dokić, V. Krstonošić, I. Nikolić, *Food Hydrocoll.* **29**, 185 (2012)
27. X. Ma, C. Chi, Y. Pu, S. Miao, D. Liu, *Food Chem.* **387**, 132876 (2022)
28. Y. Zeng, H. Zhang, Y. Guan, L. Zhang, Y. Sun, *Food Sci. Biotechnol.* **22**, 341 (2013)
29. S. Namli, S.G. Sumnu, M.H. Oztop, *Food Biosci.* **40**, 100897 (2021)
30. J.-J. Guan, A.-Y. Qiu, X.-Y. Liu, Y.-F. Hua, Y.-H. Ma, *Food Chem.* **97**, 577 (2006)
31. L. Han, S. Zhou, X. Zhang, K. Lu, B. Qi, Y. Li, *J. Food Sci.* **87**, 165 (2022)
32. S. Boostani, M. Aminlari, M. Moosavi-nasab, M. Niakosari, G. Mesbahi, *Int. J. Biol. Macromol.* **102**, 297 (2017)
33. F.-L. Gu, J.M. Kim, S. Abbas, X.-M. Zhang, S.-Q. Xia, Z.-X. Chen, *Food Chem.* **120**, 505 (2010)
34. J.T. Martins, M.A. Cerqueira, A.I. Bourbon, A.C. Pinheiro, B.W.S. Souza, A.A. Vicente, *Food Hydrocoll.* **29**, 280 (2012)
35. W.-D. Wang, C. Li, Z. Bin, Q. Huang, L.-J. You, C. Chen, X. Fu, R.H. Liu, *Int. J. Biol. Macromol.* **150**, 326 (2020)
36. Y. Du, S. Shi, Y. Jiang, H. Xiong, M.W. Woo, Q. Zhao, C. Bai, Q. Zhou, W. Sun, *J. Sci. Food Agric.* **93**, 125 (2013)
37. F. Xue, C. Li, X. Zhu, L. Wang, S. Pan, *Food Res. Int.* **51**, 490 (2013)
38. F. Zha, K. Gao, J. Rao, B. Chen, *Trends Food Sci. Technol.* **114**, 658 (2021)
39. Y. Jiang, K. Zang, R. Yan, J. Sun, X. Zeng, H. Li, C. Brennan, M. Huang, L. Xu, *Food Res. Int.* **161**, 111785 (2022)
40. G.M. Fu, Z.W. Xu, C. Luo, L.Y. Xu, Y.R. Chen, S.L. Guo, Y. Wan, *J. Biosci. Bioeng.* **132**(4), 343–350 (2021)
41. V. Schmidt, C. Giacomelli, V. Soldi, *Polym. Degrad. Stab.* **87**, 25 (2005)
42. X. Ma, W. Chen, T. Yan, D. Wang, F. Hou, S. Miao, D. Liu, *Food Chem.* **309**, 125501 (2020)
43. X. Zhu, F. Zhan, Y. Zhao, Y. Han, X. Chen, B. Li, *Food Hydrocoll.* **105**, 105758 (2020)
44. B. Amid, H. Mirhosseini, H. Poorazarang, S. Mortazavi, *Molecules* **18**, 15110 (2013)
45. M. Çelik, M. Güzel, M. Yildirim, *J. Food Sci. Technol.* **56**, 3023 (2019)
46. X. Liu, Q. Yang, M. Yang, Z. Du, C. Wei, T. Zhang, J. Liu, *Ultrason. Sonochem.* **73**, 105477 (2021)
47. Y. Xu, M. Dong, C. Tang, M. Han, X. Xu, G. Zhou, *Lwt* **117**, 108664 (2020)
48. T. Chiu, M. Chen, H. Chang, *Food Hydrocoll.* **23**, 2270 (2009)
49. E. Dickinson, E. Izgi, *Colloids Surf A Physicochem Eng Asp* **113**, 191 (1996)
50. M. Nooshkam, M. Varidi, *Food Hydrocoll.* **100**, 105389 (2020)
51. B. Wang, L. Wang, D. Li, B. Adhikari, J. Shi, *Carbohydr. Polym.* **86**, 343 (2011)
52. A. Saatchi, H. Kiani, M. Labbafi, *Int. J. Biol. Macromol.* **122**, 659 (2019)
53. W. Li, H. Zhao, Z. He, M. Zeng, F. Qin, J. Chen, *Colloids Surf. B Biointerfaces* **138**, 70 (2016)
54. Y. Wang, J. Gan, Y. Li, S. Nirasawa, Y. Cheng, *Food Hydrocoll* **87**, 129 (2019)
55. Y. Li, F. Lu, C. Luo, Z. Chen, J. Mao, C. Shoemaker, F. Zhong, *Food Chem.* **117**, 69 (2009)
56. Y. Liu, Z.-C. Wei, Y.-Y. Deng, H. Dong, Y. Zhang, X.-J. Tang, P. Li, G. Liu, M.-W. Zhang, *Molecules* **25**, 458 (2020)
57. D.J. McClements, *Crit. Rev. Food Sci. Nutr.* **47**, 611 (2007)
58. J. Sun, T. Liu, Y. Mu, H. Jing, M. Obadi, B. Xu, *Colloids Surf A Physicochem Eng Asp* **626**, 126806 (2021)
59. A. Taheri, M. Kashaninejad, A.M. Tamaddon, S.M. Jafari, *Carbohydr. Polym.* **266**, 118148 (2021)
60. T.J. Wooster, M.A. Augustin, *Food Hydrocoll.* **21**, 1072 (2007)

**Publisher's Note** Springer Nature remains neutral with regard to jurisdictional claims in published maps and institutional affiliations.